Subconductance States of a Mutant NMDA Receptor Channel
Kinetics, Calcium, and Voltage Dependence

Louis S. Premkumar, Feng Qin, and Anthony Auerbach

From the Department of Biophysical Sciences, State University of New York at Buffalo, Buffalo, New York 14214

ABSTRACT The kinetic properties of main and subconductance states of a mutant mouse *N*-methyl-D-aspartate (NMDA) receptor channel were examined. Recombinant receptors made of ζ-ϵ_2 (NR1-NR2B) subunits having asparagine-to-glutamine mutations in the M2 segment (ζN598Q/ϵ_2N589Q) were expressed in *Xenopus* oocytes. Single channel currents recorded from outside-out patches were analyzed using hidden Markov model techniques. In Ca^{2+}-free solutions, an open receptor channel occupies a main conductance (93 pS) and a subconductance (62 pS) with about equal probability. There are both brief and long-lived subconductance states, but only a single main level state. At −80 mV, the lifetime of the main and the longer-lived sub level are both ~3.3 ms. The gating of the pore and the transition between conductance levels are essentially independent processes. Surprisingly, hyperpolarization speeds both the sub-to-main and main-to-sub transition rate constants (~120 mV/e-fold change), but does not alter the equilibrium occupancies. Extracellular Ca^{2+} does not influence the transition rate constants. We conclude that the subconductance levels arise from fluctuations in the energetics of ion permeation through a single pore, and that the voltage dependence of these fluctuations reflects the modulation by the membrane potential of the barrier between the main and subconductance conformations of the pore.

KEY WORDS: single channel • substate • conductance • permeation • gating

INTRODUCTION

N-methyl-D-aspartate (NMDA)[1] receptors are cation-selective ion channels commonly found in the vertebrate central nervous system (see review by McBain and Mayer, 1994). When open, NMDA receptor channels, like many other ion channels, can assume multiple conductances (Jahr and Stevens, 1987; Stern et al., 1992; Cull-Candy and Usowicz, 1993; Gibb and Colquhoun, 1994; Stern et al., 1994). Several general mechanisms have been proposed to account for subconductance states of channels, including multiple pores (Miller, 1982; Krouse et al., 1986; Fox, 1987; Hunter and Giebisch, 1987) and fluctuations in the energetics of permeation through a single pore (Lauger, 1986; Dani and Fox, 1991).

As part of a larger study of ion transport through NMDA receptor channels, we encountered a mutant receptor that showed a prominent subconductance level (Premkumar and Auerbach, 1996*a*). This mutant is formed from mouse ζ-ϵ_2 (NR1-NR2B) subunits that each have an asparagine-to-glutamine mutation at the QRN site of the M2 segment. Several studies indicate that the channel of this mutant receptor has altered permeation properties (Burnashev et al., 1992; Sakurada et al., 1993; Ruppersberg et al., 1994; Wollmuth et al., 1996). In addition, the subconductance level of this mutant receptor channel has been shown to have a higher affinity for Ca^{2+} than the main conductance level (Premkumar and Auerbach, 1996*a*).

In this paper we address four aspects of the subconductance states of this mutant NMDA receptor. First, we describe the amplitude properties of the main and subconductance states in divalent cation-free solutions. Second, we measure the rate constants of the transitions between different conductance states of the pore. Third, we characterize the voltage dependencies of these rate constants. Fourth, we present the effects of extracellular Ca^{2+} on the kinetics of conductance level transitions. The results suggest that the receptor subconductance levels arise from fluctuations in the energetics of ion transport through a single permeation pathway, and that these fluctuations are essentially independent of the main gating event of the channel. The dependence of the fluctuation rate constants on the membrane potential indicates that voltage modulates an energy barrier that separates these channel conformations. Although Ca^{2+} binds with a higher affinity to the subconductance conformation of the channel, it does not influence the rate constants of conductance transitions. Some of these results have been presented in abstract form (Premkumar and Auerbach, 1996*b*).

Address correspondence to Dr. Anthony Auerbach, Department of Biophysical Sciences, State University of New York at Buffalo, 120 Cary Hall, Buffalo, NY 14214. Fax: 716-829-2415; E-mail: auerbach@xenopus.med.buffalo.edu

[1]*Abbreviations used in this paper:* MIL, maximum interval likelihood; NMDA, *N*-methyl-D-aspartate; SKM, segmental k-means.

METHODS

Expression

All experiments were carried out with mutant mouse ζ (NR1) and ϵ_2 (NR2B) NMDA receptor subunits having asparagine (N)-to-glutamine (Q) mutations in the M2 segment (ζN598Q/ϵ_2N589Q). A full description of the molecular biology, expression, and electrophysiology protocols is given in Premkumar and Auerbach (1996*a*). Briefly, mutant cRNAs from ζ and ϵ_2 were expressed in *Xenopus* oocytes by injection of 50 nl each of 1 μg/ml cRNAs. Oocytes were examined between 4 and 20 days after injection.

Electrophysiology

All experiments were from outside-out patches. Patch pipettes were filled with (in mM): 90 Na gluconate, 10 NaCl, 10 BAPTA, 10 HEPES (pH 7.3), 2 K_2ATP, and 0.25 GTP. The divalent cation-free extracellular solution contained: 100 NaCl, 2.5 KCl, 5 HEPES (pH 7.3), and 1.5 or 5 EGTA. The concentration of Ca^{2+} was achieved by adding $CaCl_2$ to a solution containing: 100 NaCl, 2.5 KCl, 5 HEPES (pH 7.3), and 1.5 EGTA in accordance with the computer program MAXC. The patch was continuously superfused with a solution that could be exchanged in <2 ms via a solenoid valve. The temperature was 22–25°C. To activate receptors, the perfusate was switched to one containing NMDA (10–50 μM) plus glycine (10 μM). Agonist-containing solution was applied in pulses that lasted from 5–180 s, with at least one minute between pulses.

Ultrapure NaCl, KCl, $CaCl_2$, and NaOH were obtained from Johnson Matthey (MA). NMDA, glycine, and all other reagents were obtained from Sigma Chemical Co., St. Louis (MO).

Signal Processing

Single-channel currents were recorded using an EPC-7 patch clamp amplifier (List Medical), and were stored in digital format on video tape using a data recorder (model VR-10B; Instrutech Corp., Great Neck, NY). The digitized currents were transferred to disk at a sampling frequency of either 47 or 94 kHz using a VR-111 (Instrutech) interface. The VR-10B data recorder limited the bandwidth (6 dB) to ~23 kHz. The initial channel activity was higher than the steady state level, thus for each patch the first few pulses of agonist were not acquired. Digitization of the current commenced >1 s after the initiation of each pulse, i.e., after the solution was fully equilibrated.

For analysis, the digitized current record was divided into segments. Usually, the segments were simply 5-s contiguous epochs. In some cases, segments were defined as a group of openings separated by closures of less than a critical duration, typically 50 or 1 ms. Amplitude measurements were carried out on a segment-by-segment basis. For rate constant estimation, data from several segments (but from a single pulse) were combined.

Current segments were digitally low-pass filtered (Gaussian) and resampled to the new Nyquist frequency to minimize the number of samples on the rising and falling edges of current level transitions. The filter was a zero delay Gaussian, and nonintegral decimation was achieved by interpolation. The half power frequency (f_c) values were 5–20 kHz.

Amplitude characteristics and an idealized state sequence were determined via the segmental k-means (SKM) algorithm (Rabiner et al., 1986). First, a three state Markov model was specified, with initial estimates of rate constants and amplitude parameters. The model had one state each for the closed, sub, and main conductance levels, with all states interconnected. The initial rate constants were all 1,000 s^{-1}, and the initial amplitudes were set manually. It is important to note that the detection accuracy is not sensitive to the kinetic model (the number of states for each conductance class and the starting rate constants) because the amplitude parameters dominate the likelihood function values. Next, the Viterbi algorithm (Forney, 1973; Chung et al., 1990) was used to estimate the optimal conductance level sequence, and its likelihood. The parameters of the model were then re-estimated using the amplitude and kinetic parameters of the optimal sequence, and the Viterbi algorithm was reapplied. The procedure was iterated until the likelihood stabilized, usually within five cycles. Upon convergence, an amplitude probability density was calculated from the model parameters and was superimposed on an all-points amplitude histogram of the current (see Fig. 1 *B*). In addition, a trace of the idealized conductance level sequence was displayed along with the currents, for a visual assessment of the detection accuracy. From these analyses, the mean current amplitude and standard deviation and the mean lifetime and occupancy probability for each conductance class of the model, were determined. In all figures, the continuous curves superimposed on all-points amplitude histograms (see Fig. 1 *B*) are calculated from the model parameters derived by SKM analysis.

Kinetics

Rate constants were estimated from the idealized conductance level sequences using a maximum interval likelihood (MIL) approach that had a correction for missed events (Qin et al., 1996). To minimize "edge" effects, a dead time (typically, 100 μs) was imposed. As a visual check, histograms of interval duration for each conductance class were displayed, both from the idealized currents and as calculated from the rate constants of the model. The standard deviations of the rate constants were typically within 20% of the optimal values. In all figures, the continuous curves superimposed on interval duration histograms (see Fig. 2 *B*) were calculated from the optimal rate constants, after applying a correction for missed events and sampling frequency (Qin et al., 1996).

To signal average channel openings (see Fig. 2 *C*), currents were digitized at 94 kHz and digitally low pass filtered (f_c = 1 kHz) without decimation. Opening transitions (to either the main or the subconductance level) were detected using a threshold-crossing criterion (typically set at 3 pA). Once the openings had been identified, the currents were reprocessed without any digital filtering (f_c = 23 kHz) using the previously determined threshold-crossing locations for alignment. Isolated, brief openings were excluded from the analysis.

For noise analysis (see Fig. 1 *D*), currents were sampled at 47 kHz and low pass filtered (f_c = 2 kHz). The SKM algorithm was used to identify sojourns in closed, sub, and main conductance levels that were at least 3 ms in duration. As above, the currents were reprocessed without digital filtering (f_c = 23 kHz) using the conductance transition points determined at lower bandwidth. The leading and trailing five samples of each sojourn were eliminated in order to reduce edge effects, and a 128 point fast Fourier transfer (FFT) was calculated for the remaining current samples. Up to 100 spectra for each conductance class were averaged.

RESULTS

Multiple Conductances

Fig. 1 *A* shows NMDA receptor currents, activated by 50 μM NMDA plus 10 μM glycine, obtained from an outside-out patch exposed to Ca^{2+}- and Mg^{2+}-free extracellular solution. Two open channel current levels are apparent, with amplitudes (at −90 mV) of −8.3 and −5.5 pA. We will refer to the larger current as the main level,

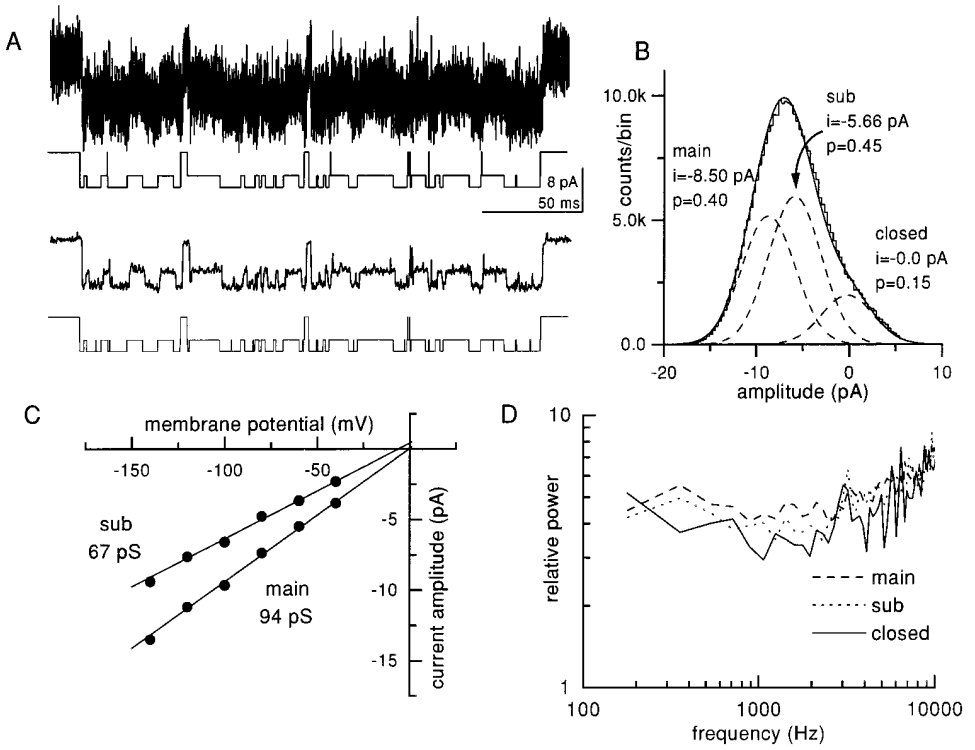

FIGURE 1. Amplitude characteristics of NMDA receptor main and subconductance levels in Ca^{2+}-free solutions. (*A*) Example currents at −90 mV (inward current is down). The top two traces are currents filtered and analyzed at 10 kHz. Main and subconductance levels of the open channel are apparent, but obscured by additive instrumentation noise. The idealized current trace was estimated using the SKM algorithm. The lower two traces show the same current filtered and analyzed at 1 kHz. The sub and main conductance levels are clearly distinguishable. (*B*) An all-points amplitude histogram of currents filtered at 10 kHz. The solid line is calculated from the final parameters of the model and is the sum of three Gaussians (dashed lines). The subconductance level has a mean amplitude (*i*) that is ~70% of the main conductance level. In this experiment, an open channel occupied either the main or sub level with about equal probability (*p*). (*C*) The current-voltage relationship for the main and subconductance levels is linear. The main level conductance is ~1.4 times greater than the sub level, but both levels reverse near 0 mV. (*D*) Spectra of the current noise for each conductance level. There is no measurable difference in the magnitudes or frequency compositions of the main and sub level currents.

and to the smaller current as the sub level. Both main and sub levels change with voltage approximately linearly, with average conductances of 93 and 62 pS, respectively (Fig. 1 *C*).

The probability of being closed varied substantially both from patch to patch, and with time in a single patch. However, once a channel opened, the relative probability that it occupied either the main or the subconductance level was consistent. Relative occupancies were determined from all-points amplitude histograms (Fig. 1 *B*). In six patches, the main conductance level was occupied with a relative probability of 0.48 ± 0.02 (range: 0.53–0.44). The relative occupancy of channels in the main and sub levels was not influenced by the external concentration of protons (pH 6.4–8.0) or NMDA (10–100 μM).

In divalent cation-free solutions, the variances of the main and sub level current noise were virtually identical, but were slightly greater than that of the closed level. To characterize the noise, we analyzed the spectrum of main, sub, and closed level currents (Fig. 1 *D*). The spectra of main and sub level currents were indistinguishable.

Kinetics

To explore the kinetics of the transitions between conductance levels, histograms were constructed of interval durations of sojourns in closed, sub, and main levels. The number of exponential components in each histogram reflects the minimum number of states for each conductance level (Colquhoun and Hawkes, 1977). The histogram for the main level was well described by a single exponential. The sub level histogram was typically described by the sum of two exponentials, although in some cases a single exponential was sufficient. Short-lived subconductance sojourns can be seen in the raw current trace shown in Fig. 2 *A*, as well as by the excess number of brief events in the interval duration histogram shown in Fig. 2 *B*. Closed interval duration histograms were quite complex and variable between patches, but could be described by the sum of two to five exponentials. There are hundreds of ways to interconnect even the minimum number of states that we observed: two closed (C), two sub (S), and one main (M). We used the following approach to select a model, without exhaustively calculating likelihood for all of the possible kinetic schemes.

In patches in which only one S and one M component were apparent, the current intervals were fitted by a kinetic model in which all three conductance classes were interconnected (solid lines in Fig. 2 *B*). In patches having two S states, we found that models with uncoupled S states yielded S-M transition rate constants that were similar to those obtained from files having a single

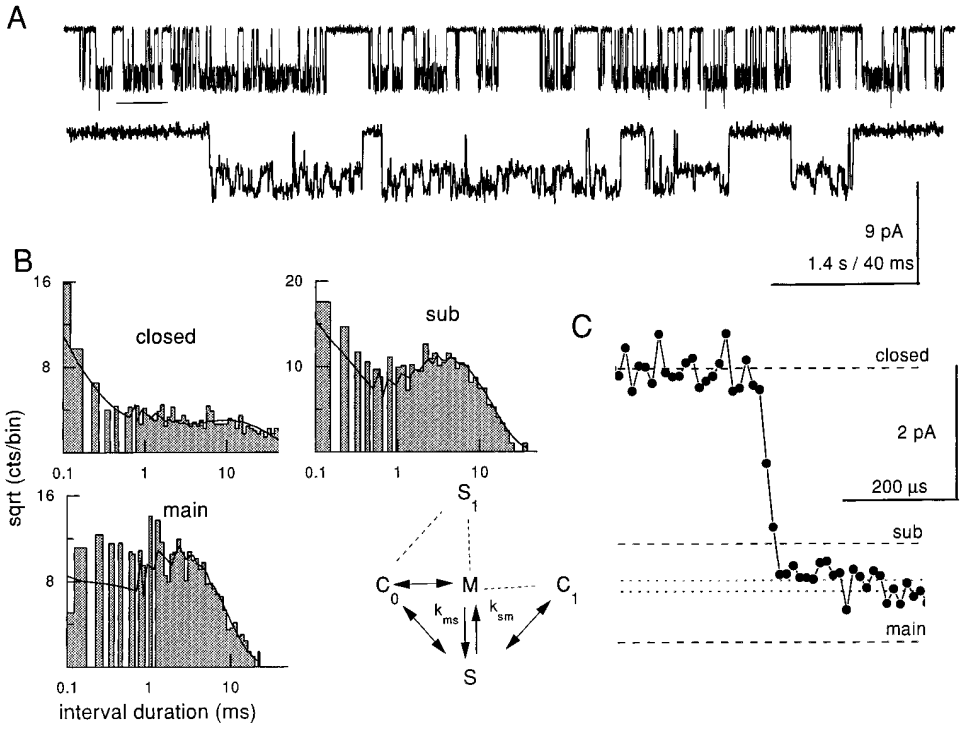

FIGURE 2. Kinetic characteristics of NMDA receptor multiple conductance levels in Ca^{2+}-free solutions. (*A*) Example currents at −80 mV. The top trace is a low time resolution view. The underlined region has been expanded in the lower trace. (*B*) Interval duration histograms and a kinetic model. The solid lines in the histograms were calculated from the optimal rate constants, estimated using the MIL algorithm. The main level histogram was described by a single exponential with a time constant (τ) equal to 2.27 ms, whereas the sub level histogram was described by the sum of two exponentials (τ_1 = 3.67 ms, 75% of all intervals; τ_2 = 0.25 ms). In this patch, the rate constant for transition from the main to the longer-lived sublevel (k_{ms}) was 328 s^{-1}, and 236 s^{-1} for the reverse transition (k_{sm}). The idealized currents were fitted by a kinetic model that had four closed, two sub, and one main level state. The solid arrows of the model represent transitions that were included in the fitting process for all patches. In some patches, additional states and transitions (indicated by dashed lines) were included (see Table I). M is the main state, S is a long-lived sublevel state, S_1 is a brief sublevel state, C_1 is a brief closed state, C_0 is a long-lived closed state; additional closed states were added in series with C_0 to describe the closed interval distribution. (*C*) Signal-averaged opening transitions of the current shown in *A*. 62 opening transitions, each following a sojourn in a closed level of at least 1 ms in duration, were aligned at the point of leaving the closed level (i.e., the first sample to cross the −3 pA threshold), and were averaged. The dashed lines indicate the amplitudes obtained from the SKM analysis for each conductance level. The dotted lines are the predicted amplitudes from the rate constants (upper line is the average of the sub and main level amplitudes, weighted by the probability of opening to either from the C_0 state; Table I), and from an all-points amplitude histogram of this patch (lower line is the average of the sub and main level amplitudes, weighted by the relative equilibrium occupancy of each level). The channel opens either the main or the subconductance level, indicating that gating and conductance fluctuations are not strongly coupled processes.

S state, while models with coupled S states did not. We therefore selected a model in which the S states were not directly connected (dashed lines in Fig. 2 *B*). We did not attempt to determine the connectivity of the C states. The two closed states were connected as shown in Fig. 2 *B*, and additional closed states were added in series to the long-lived closed state, as needed. The S-M transition rate constants did not depend on the closed state connectivity.

The average rate constants for sub-main transitions at −80 mV in pure Na^+ solutions are given in Table I. The values for the rate constants between the main state and the long-lived sub state were consistent from patch to patch. In six different patches the average sub-to-main rate constant (k_{sm}) was 287 ± 60 s^{-1}, and the average main-to-sub rate constant (k_{ms}) was 318 ± 64 s^{-1}. From the rate constants we estimate that the mean lifetime of the main level sojourn is 2.3 ms, and that of the sub level (long-lived) sojourn is 2.7 ms. In four of the six patches, a brief sub level was apparent, with an average lifetime of 0.22 ms.

Equilibrium occupancy probabilities (p) can be calculated for each state of the model. The average values of the rate constants predict that p = 0.49 for the main state, p = 0.45 for the long-lived sub state, and p = 0.01 for the brief sub state. The rate constant estimates are consistent with the observation that the relative occupancy of open channels in the main and sub levels are approximately equal. In the kinetic scheme (Fig. 2 *B*) the states C_0-S_1-M-S form a cycle. The ratio of the product of the rate constants in each direction of this cycle is 0.953. Given the error limits on the rate constants, there is no evidence to suggest that the system violates detailed balance.

In the kinetic scheme, sojourns out of the long-lived closed state (C_0) to sub or main level states may be considered to be channel opening events, i.e., to reflect the main gating event of the pore. The rate constants out of C_0 suggest that a channel opens to either sub or main levels, with perhaps a slightly greater probability of opening to a sub level (p = 0.63). Because the SKM algorithm has a tendency to associate data points on

TABLE I

Rate Constants in Ca^{2+}-free Solutions

Connection	Mean	SD	*n* Patches
$C_0 \rightarrow M$	257	164	6
$C_0 \rightarrow S$	153	67	6
$C_0 \rightarrow S_1$	288	144	4
$M \rightarrow C_0$	20	12	6
$M \rightarrow S$	**318**	**64**	**6**
$M \rightarrow S_1$	69	32	4
$M \rightarrow C_1$	39	—	2
$S \rightarrow M$	**287**	**60**	**6**
$S \rightarrow C_0$	15	8	6
$S \rightarrow C_1$	72	46	6
$S_1 \rightarrow C_0$	1494	503	4
$S_1 \rightarrow M$	3041	257	4
$C_1 \rightarrow S$	6801	2752	6
$C_1 \rightarrow M$	2794	—	2

All values are s^{-1}. The kinetic scheme is shown in Fig. 2 *B*. The state definitions are: M = main, S = long sub, S_1 = brief sub, C_0 = long closed, C_1 = brief closed. Six patches were fit; in two patches the S_1 state was not apparent, and in four patches the M-C_1 connection was not apparent. The k_{ms} and k_{ms} values are highlighted in bold. An average lifetime for each state can be calculated from the rate constants: M = 2.34 ms, S = 2.67 ms, S_1 = 0.22 ms, C_1 = 0.10 ms, $C_0 \geq 1.43$ ms. The rate constants predict that 37% of opening transitions (from C_0) will be to the main conductance level.

transitions with subconductance states, we signal-averaged channel openings (which followed closures longer than 1 ms). If channels preferentially open to a sub level, then the average current immediately after opening should be less than the equilibrium average amplitude. Conversely, if channels preferentially open to the main level, then the average current immediately after opening should be greater than the equilibrium average amplitude. The results are shown in Fig. 2 *C*. The amplitude of the average current shortly after opening is similar to that expected from the rate constants, and the average amplitude 0.25 ms after opening is close to that computed from the equilibrium occupancies estimated from an all-points amplitude histogram. These results indicate that the primary, closed-to-open gating event of the pore is essentially independent of the process that drives the transition between the main and subconductance levels.

Voltage Dependence

Fig. 3 *A* shows the effect of voltage on main-sub level transitions. As the membrane is hyperpolarized, the equilibrium occupancy of the channel does not change, but the lifetimes of both the main and the sub levels become shorter. Fig. 3 *B* shows the rate constants as a function of the membrane potential. Both k_{sm} and k_{ms} increase, approximately exponentially, with hyperpolarization. An analysis of the currents from the patch shown in Fig. 3 indicated that k_{ms} increased e-fold with a hyperpolarization of 110 mV (and is 150 s^{-1} at 0 mV), and k_{sm} increased e-fold with a hyperpolarization of 183 mV (and is 167 s^{-1} at 0 mV). A similar analysis of a different patch produced qualitatively similar results, that is e-fold increases with 92 mV (k_{ms} = 186 s^{-1} at 0 mV) and 104 mV (k_{sm} = 157 s^{-1} at 0 mV). The results indicate that the rate constants of sub-main transitions increase e-fold with ~120 mV hyperpolarization.

Effects of Ca^{2+}

Ca^{2+} blocks the current through the channel, and the concentration dependence of this block indicates that the subconductance conformation of the pore has ~35-fold higher apparent affinity for Ca^{2+} than the main conductance conformation (Premkumar and Auerbach, 1996*a*). We therefore compared the kinetics of main-sub level transitions in Ca^{2+}-free and Ca^{2+}-containing solutions. The Ca^{2+} concentrations were such that the vestibule Ca^{2+} binding was occupied with a high probability in the sub level (apparent equilibrium dissociation constant, K_d, = 5 μM), but mostly vacant in the main level (K_d = 180 μM).

Fig. 4 *A* shows currents obtained in the presence of 4.8 μM Ca^{2+}. Compared to pure Na^+ solutions, the amplitude of the sub level is reduced to a greater extent than the main level, because fast "block" of the sub level by Ca^{2+} reduces the mean channel current amplitude. At this concentration, the probability that the vestibule site is occupied by Ca^{2+} is 0.5 in the sub level, but only 0.08 in the main level. The relative probability that an open channel occupied the main level (0.45 ± 0.04, n = 5) was not altered by extracellular Ca^{2+}. In five patches, kinetic modeling was used to estimate that main-sub rate constants. In the presence of 4.8 μM Ca^{2+}, both k_{ms} (378 ± 91 s^{-1}) and k_{sm} (330 ± 47 s^{-1}) were similar to their values in Ca^{2+} free solutions.

The observed sub-to-main rate constant (k^*_{sm}) should decrease with increasing [Ca^{2+}] if a channel cannot switch conductance levels when Ca^{2+} is bound:

$$k^*_{sm} = k_{sm} / (1 + [Ca^{2+}] / K_m).$$

If, however, a channel can switch when Ca^{2+} is bound, the apparent rate constant will not vary with the extracellular [Ca^{2+}]. Fig. 4 *D* shows rate constants (at −80 mV) as a function of [Ca^{2+}]. The results indicate that under our experimental conditions, extracellular Ca^{2+} does not significantly influence the kinetic properties of the sub and main states.

DISCUSSION

Subconductance States

There are several possible mechanisms for the generation of subconductance events. One hypothesis is that a subconductance sojourn reflects unresolvably fast gating

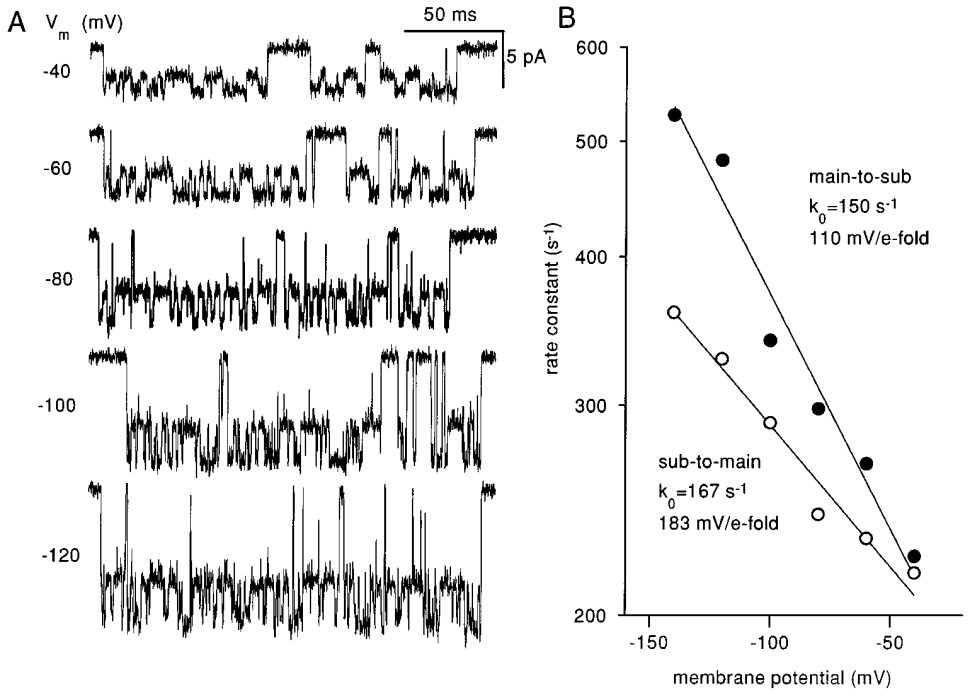

FIGURE 3. Voltage dependence of NMDA receptor conductance transitions in Ca^{2+}-free solutions. (*A*) Example currents at the indicated membrane potentials. The lifetimes of both the main and subconductance level sojourns appear to become shorter with hyperpolarization. (*B*) Rate constant estimates obtained from kinetic analysis of a single patch. The main-to-sub (k_{ms}) and sub-to-main (k_{sm}) rate constants both increase with hyperpolarization, suggesting that voltage influences the height of a barrier separating the conformations that generate the main and sub conductances.

events, i.e., rapid transitions between fully closed and fully open (main) states. If so, such sublevel flickering must be voltage independent because the current voltage relationship is linear (Fig. 1 *C*). In addition, it must be extraordinarily fast because there is no measurable excess noise in the sub level compared to the main level (Fig. 1 *D*).

We can quantify how fast the flickering needs to be based on the excess variance it would be expected to produce. The spectral density of a two-state process can be estimated as (FitzHugh, 1983):

$$S(\omega) = \frac{2I_m^2 k_{co} k_{oc}}{(k_{co} + k_{oc})^3} \cdot \frac{1}{\left(1 + \frac{\omega}{k_{co} + k_{oc}}\right)^2},$$

where k_{co} and k_{oc} are the opening and closing rate constants and I_m is the amplitude of the main state. The mean amplitude of the process (i.e., the measured subconductance amplitude), I_s, is given by:

$$I_s = I_m k_{co} / (k_{co} + k_{oc}) .$$

Thus, the excess variance produced by flickering is approximated by:

$$\sigma_{ex}^2 = S_f(0)\, B = 2BI_s (I_m - I_s) / (k_{co} + k_{oc}) ,$$

where B is the bandwidth.

Experiments in Ca^{2+}-free solutions indicate that the sublevel variance is not detectably larger than the main level variance (Fig. 1 *D*). Nonetheless, we estimate that the accuracy of these measurements of variance was such that $\sigma^2_{ex} \leq 0.02$ pA^2 when $B = 10$ kHz, i.e., $(k_{co} + k_{oc})^{-1} \leq 86$ ns. For rapid gating to account for subconductance states, such events must take place on the same time scale as ion translocation events. The lack of excess noise in the sub level leads us to reject the hypothesis that fast gating accounts for NMDA receptor subconductance states.

A second hypothesis is that subconductance levels arise from the gating of multiple permeation pathways. This concept has been used to describe the gating between of multiple conductances of a Cl^--selective channel from *Torpedo* (Miller, 1982) and of other channels (Krouse et al., 1986; Hunter and Giebisch, 1987). For example, in mutant NMDA receptors the 94 pS "main" level could reflect current flow through two open pores (67 and 27 pA), whereas sub levels reflect times when only the larger conductance pore is open. The fact that main and sub level pore currents both reverse at 0 mV (Fig. 1 *C*) indicates that both pores have similar equilibrium potentials.

Two relevant observations are that the Ca^{2+} equilibrium dissociation constant is ~35 times higher in the main level compared to the sub level, and that binding Ca^{2+} results in a nearly complete block of the current through the subconductance pore (Premkumar and Auerbach, 1996*a*). According to the multiple pore hypothesis, the sub level reflects a single, open, high Ca^{2+} affinity pore, whereas the main level represents two open pores, only one of which has a high affinity for Ca^{2+}. Thus, according to this hypothesis, at −80 mV, concentrations of Ca^{2+} well above the K_d of the high affinity pore should virtually abolish the sub level current, and reduce the main level current to ~2 pA (i.e., the residual conductance of the low affinity pore). This is inconsistent with the experimental observations,

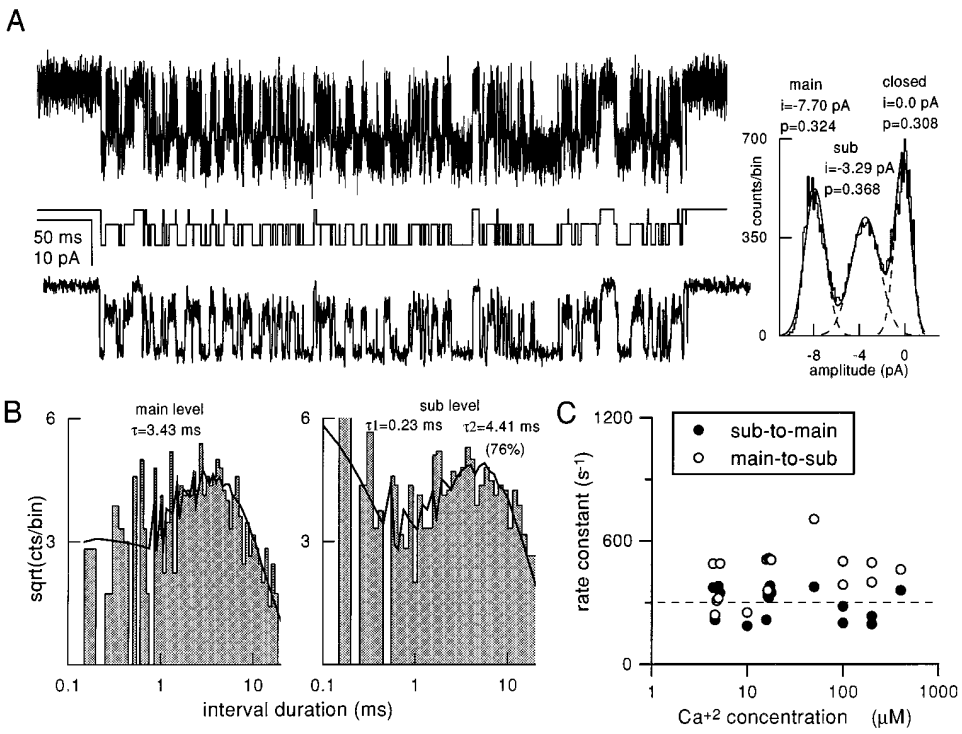

FIGURE 4. Effects of Ca^{2+} on the rate constants of conductance transitions. (*A*) Example currents obtained in the presence of 4.8 μM extracellular Ca^{2+} (−80 mV). The top trace was filtered at 10 kHz, the middle trace is the idealization of the top trace using the SKM algorithm, and the lower trace is the same current filtered at 1 kHz. The all-points amplitude histogram (1 kHz filtering) is shown at the right. Ca^{2+} concentration only modestly affects the amplitude of the main level, but lowers that of the sub level to about half of the amplitude in pure Na^+ solutions because of unresolved channel block. (*B*) Main and sub level interval duration histograms for the patch shown in *A*. Even though the sublevel was occupied by Ca^{2+} about half of the time, the main-sub level transition rate constants (k_{ms} = 239 s^{-1}, and k_{sm} = 213 s^{-1}) were similar to those obtained in Ca^{2+}-free solutions (see Table I). (*C*) Rate constants as a function of extracellular Ca^{2+}. At each concentration, each symbol is from a different patch. The rate constants show little, if any, dependence on the external Ca^{2+}.

which show that Ca^{2+} indeed blocks the sub level but leaves the main level virtually untouched (Fig. 4 *A*; Premkumar and Auerbach, 1996*a*). Because the sub level has a higher affinity for Ca^{2+}, we reject the hypothesis that subconductance states of NMDA receptors arise from the gating of multiple independent ion conductance pathways.

A third hypothesis is that subconductance states reflect fluctuations in the free energy profile for the permeation of ions through a single channel structure (Auerbach and Sachs, 1983; Lauger, 1986). That is, Na^+ passes through the NMDA pore ~30% more slowly during sub level sojourns because it encounters relatively higher energy barriers and/or deeper wells during its transit.

This hypothesis is consistent with the experimental results. It predicts that the current noise should decrease, rather than increase, with the lower sub level current, as was observed. Ca^{2+} flows through the sub level conformation ~40 times slower than through the main level conformation because it remains bound to a site near the pore entrance for a relatively long time (35 vs. 0.9 μs; Premkumar and Auerbach, 1996*a*). By elimination, we conclude that the difference in conductance between main and subconductance state of NMDA receptors arises from changes in the permeation properties of a single pore. Our experiments do not provide information whether multiple conductances arise from fluctuations in energy wells and/or barriers in the permeation pathway.

Signal averaging opening transitions shows that the average current immediately after a transition (i.e., within about 30 μs) is similar to the steady-state amplitude (Fig. 2 *C*), and single-channel kinetic analyses indicate that channels can open to either the main or to sub level states (Table I). These results suggest that the events that underlie gating and the conductance fluctuations of the pore are essentially independent processes. The aggregate rate at which a channel exits the long-lived closed state (C_0) to either a sub or main conductance level is an estimate of the NMDA receptor channel opening rate, which we calculate to be 698 s^{-1} for these mutant receptors.

Voltage Dependence

The rate constants for the subconductance level transitions show an unusual voltage dependence: both forward and reverse rate constants increase exponentially with hyperpolarization (Fig. 3 *B*). The similar polarity of the voltage dependencies indicates that the membrane potential does not influence the relative stability of either the main or sub level conformations. This suggests that the salient charges are in the same relative position with respect to the electric field. Changing the membrane potential appears to change the height of

an energy barrier that separates the main and subconductance configurations of the channel. Hyperpolarization lowers the barrier allowing main and sub level configurations of the pore to interconvert more rapidly, but does not alter the equilibrium occupancy of the conductance levels.

The pattern of voltage dependence suggests that the sub-main transition requires the net movement of charge, but that the initial and final positions of the center of charge is in the same position relative to the electric field in the sub and main states. For example, the sub-main conformational change may involve a rotation or tilt of subunits or sidechains, with the center of charge not shifting between the end states, but shifting in the transition state. Assuming that the field is normal to the axis of the particle rest positions, the magnitude of the voltage dependence of the sub-main switching rate constants is the product of the fraction of the electric field (δ) and the magnitude of the charge (z). The voltage dependence of k_{sm} and k_{ms} are approximately equal ($\sim$122 mV/e-fold change), indicating that $z\delta \cong 0.20$ for each direction of the transition.

Physical Interpretation

The following picture emerges of the pore of NR1-NR2B NMDA receptors having an asparagine-to-glutamine mutation in the M2 segment of each subunit. The open pore can assume two stable structures, main and sub. Other conductance levels are not apparent. At -80 mV and 23°C, the main and sub structures interconvert about every 3 ms. This corresponds to an energy barrier of $\sim$14 kcal/mol separating the two structures. The probability that the channel assumes a sub or main structure is essentially independent of the gating status of the channel. Although the membrane potential modestly influences the rate constants for the conductance transition (by $\sim$0.5 kcal/mol, in the physiological range of voltages), the equilibrium probability that the channel assumes a sub or main structure is independent of voltage. The evidence indicates that the fluctuation in structure is an intrinsic aspect of the mutant receptor protein that is quite immune to environmental perturbation.

Wild-type NMDA receptors do not exhibit a prominent subconductance level in Ca^{2+}-free solutions. The fact that mutant receptors occupy a sub level with a relatively high probability can therefore be attributed to one or more of the mutated (glutamine) residues. Our experiments do not allow us to determine if the change in conductance is due to changes in the disposition of the glutamine residues themselves, or whether the glutamines alter the properties of the protein at some distance. We also do not know if a specific subset of the glutamine residues induce the conductance fluctuations of the pore, or if all of the glutamines act in a concerted fashion to alter the conductance.

The subconductance conformation of the pore is characterized by a lower Na^+ current. Previous work (Premkumar and Auerbach, 1996*a*) has shown that this conformation is also characterized by a higher Ca^{2+} affinity, as this ion lingers at a site that is, on average, $\sim$15% through the electric field from the extracellular solution. One may consider the possibility that the site that binds Ca^{2+}, and the site that limits the Na^+ current, are one-and-the-same, i.e., that the structural elements of the pore that fluctuate between main and sub configurations are identical to those that bind these cations. A major problem with this hypothesis is that Ca^{2+} does not alter the rate constants of the sub-main transitions. The coordination of a divalent cation almost certainly would alter the free energy of a conformational change that involved the coordinating ligands, yet there is almost no effect of Ca^{2+} on the main-sub transition rate constants (Fig. 4 *C*). It is therefore unlikely that the mutated residues constitute the high affinity divalent cation binding site. Rather, these residues may serve as a barrier for the permeation of cations, with the fluctuations in Na^+ conductance and Ca^{2+} affinity arising from fluctuations in the height of this barrier. Permeation in NMDA receptors is determined both by interactions of cations with a superficial binding site, and at a constriction, formed by QRN residues, that lies deep within the electric field of the membrane (Villarroel et al., 1995; Zarei and Dani, 1995; Kuner et al., 1996).

In conclusion, subconductance levels of NMDA receptors arise from fluctuations in a barrier to ion permeation through a single pore. The unusual voltage dependence of these fluctuations reflects the modulation by the membrane potential of a transition state, rather than a change in the stability of either the sub or main conductance conformation. The structural correlates of these functional characteristics remain to be determined.

We thank M. Mishina for the subunit cDNAs, and K. Lau for molecular biology technical assistance. We also thank L. Wollmuth, F. Sigworth, and C. Miller for comments on the manuscript.

Supported, in part, by National Institutes of Health grants NS-23513 and RR-11114.

Original version received 1 August 1996 and accepted version received 4 November 1996.

REFERENCES

Auerbach, A., and F. Sachs. 1983. Single-channel currents from acetylcholine receptors in embryonic chick muscle: kinetic and conductance properties of gaps within bursts. *Biophys. J.* 45:187–198.

Burnashev, N., R. Schoepfer, H. Monyer, J.P. Ruppersberg, W. Gunther, P.H. Seeburg, and B. Sakmann. 1992. Control by asparagine residues of calcium permeability and magnesium blockade in NMDA receptor. *Science (Wash. DC).* 257:1415–1419.

Chung, S.H., J.B. Moore, L. Xia, L.S. Premkumar, and P.W. Gage. 1990. Characterization of single channel currents using digital signal processing techniques based on Hidden Markov Models. *Philos. Trans. R. Soc. Lond. B. Biol. Sci.* 329:265–285.

Colquhoun, D., and A.G. Hawkes. 1977. Relaxation and fluctuation of membrane currents that flow through drug-operated channels. *Philos. Trans. R. Soc. Lond. B. Biol. Sci.* 199:231–262.

Cull-Candy, S.G., and M.M. Usowicz. 1993. On multiple-conductance single channels activated by excitatory amino acid in large cerebellar neurons of the rat. *J. Physiol. (Lond.).* 415:555–582.

Dani, D.A., and J.A. Fox. 1991. Examination of subconductance levels arising from a single ion channel. *J. Theor. Biol.* 153:401–423.

FitzHugh, R. 1983. Statistical properties of the asymmetric random telegraph signal, with applications to single-channel analysis. *Methods Biosci.* 64:75–89.

Forney, G.D. 1973. The "Viterbi algorithm." *Proc. IEEE.* 61:268–278.

Fox, J.A. 1987. Ion channel subconductance states. *J. Membr. Biol.* 97:1–8.

Gibb, A.J., and D. Colquhoun. 1994. Activation of N-methyl-D-aspartate receptor by L-glutamate in cells dissociated from adult rat hippocampus. *J. Physiol. (Lond.).* 456:143–179.

Hunter, M., and G. Giebisch. 1987. Multi-barreled K channel in renal tubules. *Nature (Lond.).* 327:522–524.

Jahr, C.E., and C.F. Stevens. 1987. Glutamate activates multiple single channel conductances in hippocampal neurons. *Nature (Lond.).* 325:522–528.

Krouse, M.E., G.T. Schneider, and P.W. Gage. 1986. A large anion-selective channel has seven conductance levels. *Nature (Lond.).* 319:58–60.

Kuner, T., L.P. Wollmuth, A. Karlin, P. Seeburg, and B. Sakmann. 1996. Structure of the NMDA receptor channel M2 segment inferred from the accessibility of substituted cysteines. *Neuron.* 17: 343–352.

Lauger, P. 1986. Ion channels with conformational substates. *Biophys. J.* 47:581–591.

McBain, C.J., and M.L. Mayer. 1994. N-Methyl-D-Aspartic acid receptor structure and function. *Physiol. Rev.* 74:723–760.

Miller, C. 1982. Open-state substructure of single chloride channels from Torpedo electroplax. *Philos. Trans. R. Soc. Lond. B. Biol. Sci.* 299:401–411.

Premkumar, L.S., and A. Auerbach. 1996*a*. Identification of a high affinity divalent cation binding site near the entrance of the NMDA receptor channel. *Neuron.* 16:869–880.

Premkumar, L.S., and A. Auerbach. 1996*b*. Voltage-dependence switching between sub and main conductance levels in recombinant mutant NMDA receptors channels. *Biophys. J.* 70:A75. (Abstr.)

Qin, F., A. Auerbach, and F. Sachs. 1996. Estimating single-channel kinetic parameters from idealized patch-clamp data containing missed events. *Biophys. J.* 70:264–280.

Rabiner, L.R., J.G. Wilpon, and B.H. Juang. 1986. A segmental k-means training procedure for connected word recognition. *AT&T Tech. J.* 65:21–31.

Ruppersberg, J.P., J. Mossbacher, W. Gunther, R. Schoepfer, and B. Fakler. 1993. Studying block in cloned N-methyl-D-aspartate (NMDA) receptors. *Biochem. Pharmacol.* 46:1877–1885.

Sakurada., M. Masu, and S. Nakanishi. 1993. Alteration of Ca^{2+} permeability and sensitivity to Mg^{2+} and channel blockers by single amino acid substitution in the N-methyl-D-aspartate receptor. *J. Biol. Chem.* 268:410–415.

Stern, P., P. Behe, R. Schoepfer, and D. Colquhoun. 1992. Single-channel conductances of NMDA receptors expressed from cloned cDNAs: comparison with native receptors. *Proc. R. Soc. Lond. B. Biol. Sci.* 250:271–277.

Stern, P., M. Cik, D. Colquhoun, and A.F. Stephenson. 1994. Single channel properties of cloned NMDA receptors in a human cell line: comparison with results from Xenopus oocytes. *J. Physiol. (Lond.).* 476:391–397.

Wollmuth, P.L., T. Kuner, P.H. Seeburg, and B. Sakmann. 1996. Differential contribution of the NR1- and NR2A- subunits to the selectivity filter of recombinant NMDA receptor channels. *J. Physiol. (Lond.).* 491:779–797.

Villarroel, A., N. Burnashev, and B. Sakmann. 1995. Dimensions of the narrow portion of a recombinant NMDA receptor channel. *Biophys. J.* 68:866–875.

Zarei, M.M., and J. Dani. 1995. Structural basis for explaining open-channel blockade of the NMDA receptor. *J. Neurosci.* 15:1446–1454.